Journal of Alloys and Compounds 495 (2010) 131–137

Contents lists available at ScienceDirect

Journal of Alloys and Compounds

journal homepage: www.elsevier.com/locate/jallcom

Spectroscopic and thermal characterization of tetrathiomolybdate-organic amine homologous systems

Suman Pokhrel*, K.S. Nagaraja

Loyola Institute of Frontier Energy, Loyola College, Chennai 600034, India

ARTICLE INFO

Article history:
Received 10 November 2009
Received in revised form 19 January 2010
Accepted 21 January 2010
Available online 1 February 2010

Keywords:
Tetrathiomolybdates
Organic amines
Single crystals
Thermal properties

ABSTRACT

The homologous series of organic–inorganic hybrid single crystals (diethylenetriamine-H_2-MoS_4—**I**, triethylenetetramineH_2-MoS_4—**II** and 1,4-diazobicyclo-2,2,2-octaneH-NH_4-MoS_4—**III**) were prepared by passing hydrogen sulfide gas in the aqueous solution of ammonium heptamolybdate and their respective amines. These crystals were analysed using Fourier Transform-Infrared (FT-IR), UV–vis and ^{1}H NMR spectroscopy. The discrepancies in the bond angles and bond lengths have been theoretically explained in terms of hybridisation variations. The thermal analytical techniques such as TG/DTG and DSC were used to study thermal properties at high and low temperatures. DSC at low temperature suggested reversible solid–solid transitions and the respective ΔH, ΔS and ΔG have been derived. SEM analysis of the crystals showed the sedimented smooth layers of these sulfido-metallic crystals before heat treatment were converted into fine powder with tiny capillary pores in the bulk after thermal treatment.

1. Introduction

The importance of molybdenum–sulfur chemistry in industrial catalysis and bioinorganic chemistry has stimulated recent interest inducing broad research in these fields [1–4]. Many of the new sulfidometal complexes prepared and characterized, in the recent years, have revealed novel structures and bonding modes. The binary Mo–S anions such as MoS_4^{2-}, $Mo_2S_8^{2-}$, $Mo_2S_{12}^{2-}$, $Mo_3S_9^{2-}$, [5–7] have unusual stoichiometries, oxidation states and coordination geometries. A variety of structurally diverse Mo–S compounds have been synthesized using $[MoS_4]^{2-}$ precursor with the appropriate organic/inorganic precursors as a building block for the synthesis of several novel Mo–S inorganic complexes [8,9] and inorganic pathways [10]. The bioavailable Mo–S when enters the cell, is subsequently incorporated by complex biosynthetic machineries into metal cofactors [11,12]. All enzymes depend on molybdenum catalyze redox reactions by taking advantage of the versatile redox chemistry of the molybdenum [13]. In nature, two very different systems have been developed to control the redox state and catalytic power of molybdenum, which functions as an efficient catalyst in oxygen-transfer reactions. In either case, at least three S and two O atoms form ligand to molybdenum which is typical for molybdenum nitrogenase [14]. Moreover, the use of tetrathiomolybdate for the treatment of metastatic cancer has added an entire new dimension to the chemistry of these ions [15,16].

In this report, we have synthesized, spectroscopically and thermally characterized water soluble organic amine-MoS_4^{2-} single crystals. We have also tried to explain the abnormalities in the bonding modes of these hybrid systems through fractional differences between sp^2 and sp^3 hybridisations. To the best of our knowledge, no reports on thermal treatment (at low temperature) of these systems are found. We have attempted to make this study on few of our crystals whose structure has been determined. Since it is very interesting to see how organic amine and inorganic $[MoS_4]^{2-}$ materials respond to thermal treatment, we hereby report the spectroscopic and analytical characterization of these single crystals for better understanding of the bonding modes and charge-transfer transitions between the coordinating amine and the thiochelate.

2. Experimental details

2.1. Preparation of (amine-MoS_4) single crystals [dienH_2-MoS_4 (**I**), trienH_2-MoS_4 (**II**) and 1,4-diazobicycloamineH-NH_4-MoS_4 (**III**)]

The detail experimental techniques have been described elsewhere [17–19]. In short, a steady stream of H_2S gas was passed through the aqueous ammonium heptamolybdate (3 g, E Merck) in water (30 cm^3) containing organic amine (8 cm^3 99% pure, E Merck) for 2 h at 50 °C. The immediate brown precipitate obtained was dissolved in continuous flow of H_2S gas. The resulting blood red solution was filtered and allowed to stand at 15 °C for 1 h. The crystals were filtered, washed with ice-cold water/isopropanol/petroleum ether and dried under vacuum. The yield after recrystallization in hot water (70–80 °C) was found to be 70–75%.

* Corresponding author. Present address: Foundation Institute of Material Science, University of Bremen, Badgasteiner Str. 3, 28359 Bremen, Germany.
Tel.: +49 421 218 2780; fax: +49 421 218 5401/5378.
E-mail address: spokhrel@iwt.uni-bremen.de (S. Pokhrel).

0925-8388/$ – see front matter © 2010 Elsevier B.V. All rights reserved.
doi:10.1016/j.jallcom.2010.01.101

2.2. Instrumentation

The IR spectra were recorded in the PerkinElmer RXI FT-IR spectrophotometer after pressing the samples with KBr. UV–vis spectrums were recorded using the PerkinElmer Lambda 3B UV-Visible spectrophotometer. The protons NMR spectral analyses of the organic amine based terathiomolybdates in D_2O were carried out using JEOL GSX-400 NMR instrument at swiping frequency of 400 Hz cm^{-1} at ambient temperature. TG and DSC analysis was performed in PerkinElmer thermal analyzer (TGA 7) in ambient air and NETZSCH DSC 204 instrument in nitrogen atmosphere. The furnace is supplied with a silver block assisted by a miniature-jacketed heater where the temperature is monitored periodically by a thermocouple integrated into the furnace wall. The sample chamber has two silver lids one for the sample and the other for reference. The instrument further comprised a cooling unit where there was a provision for liquid nitrogen, air and refrigeratory bath (circulatory) for the low temperature measurements. The sample ≈ 6.5 mg was closed in Al_2O_3 sample chamber and kept in the heating unit for thermal measurements. The X-ray diffraction patterns were obtained with a Phillips diffractometer using CuK_α radiation. The samples were then pressed on a glass plate with a well of depth 1 mm.

3. Results and discussion

3.1. Stability

The crystals **I**, **II** and **III** [Fig. 1(a)–(c)] were left in the open air and the blood red colour slowly changed to black in 15, 35 and 60 days respectively due to the exchange of sulfur with oxygen in the samples. It has been reported [20,21] that ammonium tetrathiomolybdate slowly decomposes in air by induced electron transfer process resulting in the formation of $[Mo_2O_2S_6]^{2-}$ species and the process is quite facile under room temperature. Therefore, the crystals had to be stored under N_2 atmosphere to avoid deterioration to facilitate their use at a latter time. The relative stability of **III** compared to those of **I** and **II** could be ascribed to the bonding of MoS_4^{2-} through rigid bicyclic amine with strong H-bonds [see Fig. 1(c)]. Though the hydrogen bonding networks were present in all the three crystals, the lower stabilities are suggested due to the flexibility of the linear amines in contrast to the rigidity accrued by cyclic amine.

3.2. Infrared spectroscopy

The FT-IR intense bands positions occurring at 3078.2, 3065.5 and 3057.2 cm^{-1}, for **I**, **II** and **III** are attributed to the $\nu(N–H)^+$ evidencing the molecular interactions between the organic and inorganic moieties (Fig. 2). It has also been observed that the terminal rather than the central N–H understandably participates in H-bonding. The ν(C–H) for all the three crystals occurred at 1446.5, 1441.1, and 1444.2 cm^{-1} respectively. The infrared bands at 1114.8, 1128.4, and 1045.6 cm^{-1} for **I**, **II** and **III** are attributed to ν(C–N) vibration of the amines. In the case of linear amines bending/stretching is easier than that in cyclic amine where the bending/stretching could result in angle strain to a considerable extent. For this reason the ν(C–N) frequency occurs at the higher region as compared to those of **I** and **II** obviously occurring at a lower region. The band at 474.5, 474.1 and 481.6 cm^{-1} for **I**, **II** and **III** could be attributed to the presence of ν(Mo=S) asymmetric vibration due to MoS_4^{2-} moiety. The infrared spectrum of $Mo_2S_4^{2+}$ core was reported to correspond to ν(Mo=S) at 523 cm^{-1} and a series of weaker bands between 496 and 296 cm^{-1} differing substantially from the infrared spectrum exhibited by $Mo_2S_{12}^{2-}$ anion [1,10]. Recently it has been reported that the ν(Mo–S) band for the doubly bridged and double cubane cluster complex of $[MoFe_3S_4]$ exhibits

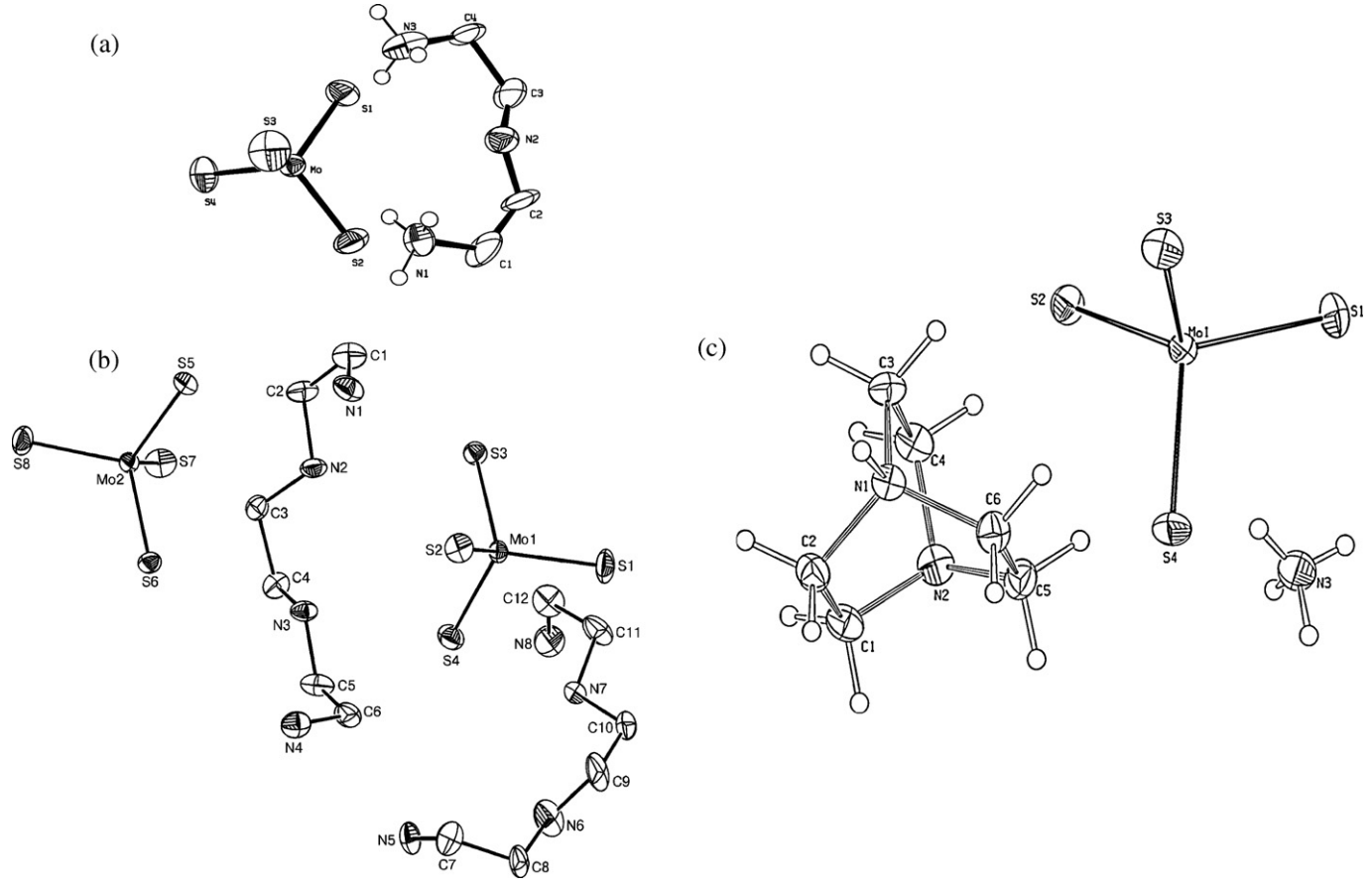

Fig. 1. ORTEP structures of (a) diprotonated diethylene triammonium tetrathiomolybdate [$dienH_2$][MoS_4], (b) diprotonated triethylene tetraammonium tetrathiomolybdate [$trienH_2$][MoS_4] and (c) Protonated 1,4-diazo-bicyclo-2,2,2-octane ammonium tetrathiomolybdate [NH_4][DABCOH][MoS_4].

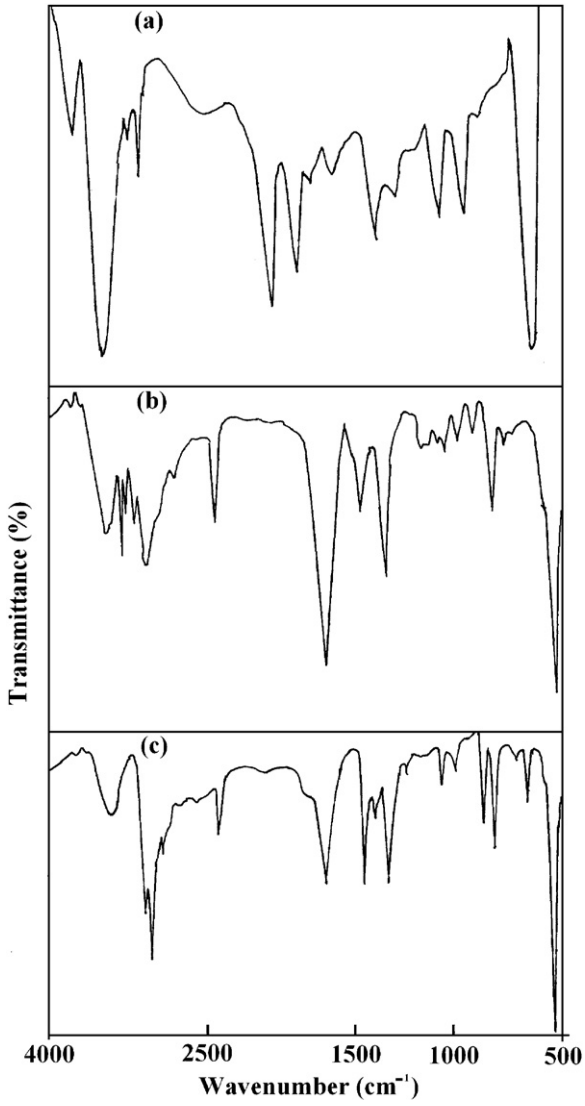

Fig. 2. FT-IR spectra of (a) $[dienH_2][MoS_4]$, (b) $[trienH_2][MoS_4]$ and (c) $[NH_4][DABCOH][MoS_4]$.

a band [22] at 408 cm^{-1} and the same band for $MoO_2S_2^{2-}$ occurs [23] at 466 cm^{-1}.

3.3. UV–vis spectroscopy

The structural bonding of the tetrahedral molybdate systems has been well described employing molecular orbital (MO) approach [24]. The thio-ligands are expected to be involved in both sigma and π-bonding with Mo. The difference between the $3t_2$ and 2e levels represents the Δ_t value for the system. Since there are no *d*-electrons, this splitting is not attainable from the analysis of *d–d* transitions. It can however, be estimated from the difference in the energy associated with the charge-transfer bands. Thus the difference between ν_3 and ν_1 is found to correspond to the value of Δ_t. The three UV–vis absorptions [Fig. 3(a)–(c)] of the ammonium tetrathiomolybdate occurring at 21,400, 31,500 and 41,300 cm^{-1} corresponds to $\nu_1(t_1 \rightarrow 2e)$, $\nu_2(2t_2 \rightarrow 2e)$ and $\nu_3(t_1 \rightarrow 3t_2)$ transitions. The UV–vis spectra of the crystals based on tetrathiomolybdates have the peaks at 469 nm (21,321 cm^{-1}), 315 nm (31,746 cm^{-1}) and 240 nm (41,666 cm^{-1}) for **I**, 470 nm (21,276 cm^{-1}), 320 nm (31,250 cm^{-1}) and 240 nm (41,666 cm^{-1}) for **II** and 465 nm (21,505 cm^{-1}), 330 nm (30,303 cm^{-1}) and 240 nm (41666 cm^{-1}) for **III**. The marginal difference in the wavelength is explained due to the variation in linear and cyclic nature of amine cations.

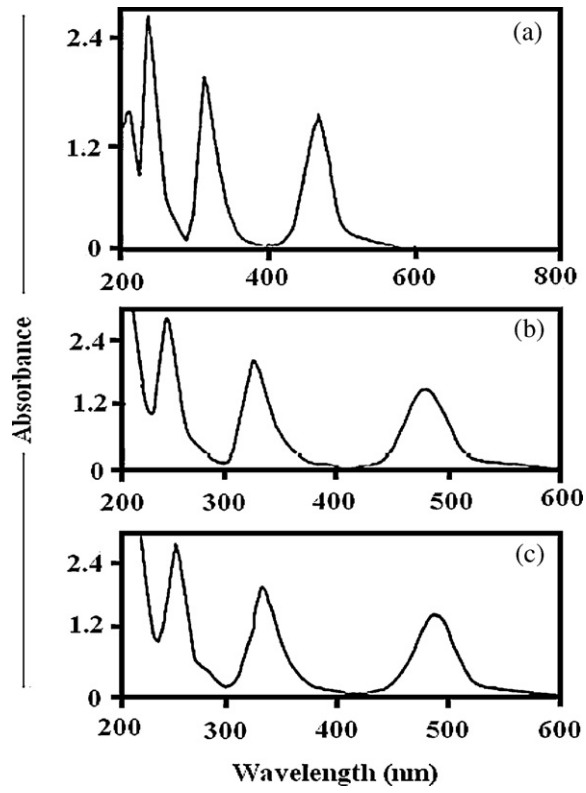

Fig. 3. UV–vis spectra of (a) $[dienH_2][MoS_4]$, (b) $[trienH_2][MoS_4]$ and (c) $[NH_4][DABCOH][MoS_4]$.

3.4. Proton NMR (^{1}H NMR) spectroscopy and crystal structure

The ^{1}H NMR of pure diethylenetriamine (for figure see Ref. [17]) molecule showed the two sets of triplets at δ values of 2.58 and 2.92 ppm with the separation of 0.34 ppm. The triplet at 2.58 ppm is due to the equivalent C1 and C3 whereas another set of triplet occurring at 2.92 ppm is due to equivalent C2 and C4 protons. The protons in the nitrogen atoms are exchanged rapidly with the deuterium atom from D_2O with broad peak attributing the protons in the nitrogen atoms. The spectrum of aqueous solution of the crystal showed presence of two sets of multiplets rather than the triplets expected. These A_2B_2 multiplets of the two equivalent protons are exactly the mirror image to one another explaining the magnetic equivalence of the two sets of $-CH_2$ groups. Though protons in the two different nitrogen (two terminal and one central) atoms also interact with the $-CH_2$ protons, the two symmetrical multiplets were not to be expected. One $-CH_2$ (A) gives rise to a sexet at δ value of 2.9 and another set (B) gives similar sexet at 3.1 ppm. The ^{1}H NMR of $(trienH_2)(MoS_4)$ showed one singlet at 2.64 ppm and the two triplets at 2.74 and 2.86 ppm. The triplets were symmetrical as in the case of diethylenetriamine tetrathiomolybdate. The protons from $(trienH_2)$ gave rise to a triplet and a similar triplet obtained from those protons from the $(trienH_2)'$ coincides with one another forming AA′BB′ spectral system. The ^{1}H NMR of $(NH_4)(DABCOH)(MoS_4)$ single crystal in D_2O (for figure see Ref. [18]) comprises of one single peak with a small broad peak at δ value of 3.5 and 4.5 ppm respectively. It is found that the shifting of the singlet present in the DABCO molecule and the complex was 0.99 ppm. The DABCO molecule consists of three $-CH_2-CH_2-$ groups situated at three different orientations and comprised of

$6m_2$ symmetry. When the molecule is rotated by a twofold or threefold axis the molecular arrangement is the same. This is the reason why all the three $-CH_2-CH_2-$ groups are equivalent and all the protons in each carbon atom give rise to a single peak along with a broad peak corresponding to the protons in the nitrogen atoms. When $(NH_4)^+(DABCOH)^+$ and $(MoS_4)^{2-}$ are hydrogen bonded as evidenced from the single crystal analysis, it is found that only one of the N-atom of the bicyclic ligand is protonated. This should bring the change in the ^1H NMR spectra, which is not observed. The proton attached in one of the nitrogen atom is exchanging between the two nitrogen atoms making the entire carbon atoms once again equivalent. The ^1H NMR spectra of the $(NH_4)(DABCOH)(MoS_4)$ is found to be identical to that of the pure bicyclic amine.

The discrepancies in the bond angle and bond length (especially with C–C, C–N and N–C–C) described in the literature [19–21] and the ^1H NMR patterns are explained for dienH_2-MoS_4 as a case study and the same applies for trienH_2-MoS_4 also. The bond distances between N2–C3 and C3–C4 are 1.290 and 1.577 Å with the bond angle N2–C3–C4 being 124.10° (sp^2) rather than the expected tetrahedral angle for crystal **I** (see Fig. 1). The short bond distance N2–C3 is attributed to the probable orbital overlap (sp^2) of N2 with C3 where the lone pair in N2 occupies a *p*-orbital assuming the hybridisation of $sp^2 + p$ rather than pure sp^3 as expected. The C3–C4 bond distance is longer because of the decrease in the *s*-character leading to a lesser overlap. Since N2 has used more *p*-character towards C3 for its overlap, the N2–C2 bond distance (1.442 Å) becomes longer as N2 uses orbital with less *p*-character and more *s*-character for overlapping with C2. C2 in turn exercises more *p*-orbital overlap with C1 making the shorter bond length and angle of 1.36 Å and 121.2°; hybridisation being $sp^2 + p$ rather than sp^3. The similar case of bond angle and bond length differences are also observed in the aminobenzoquinones [25]

The tetrathiomolybdate anion is bonded more to N1 hydrogen than that with N3 hydrogen. Thus the amine cation has been distorted giving N1–C1–C2 angle of 121.2° suggesting sp^2 for C1 whereas 106.2° for N3–C4–C3 suggesting C4 with more *s*-character especially towards C3 with the bond distance C4–C3 being 1.577 Å. In fact from the single crystal structure, two different ^1H NMR signals for C2 and C3 carbon atoms may be expected because the N2–C3 and N2–C2 bond distances are different. This is probably due to the fact that N2–C2 and C2–C1 bond lengths are long and short whereas N2–C3 and C3–C4 bond lengths are short and long respectively. Thus C2 and C3 have similar orbital with more $sp^2 + p$-character disposed towards H-atom making them equivalent which is expected to come at a higher δ value (3.1) when compared to the H-atoms attached to C1 and C4 atoms (2.9).

3.5. Thermal gravimetric (TG) analysis

The crystals were heat treated in the range of 50–800 °C at the heating rate of 5 °C/min. The thermal analysis [Fig. 4(a)] of **I** showed that the compound starts decomposing at 110 °C and the weight loss in the temperature range 500–800 °C was found to be very slow. The weight loss in the sample was found to occur in two steps. The first step involved the mass loss of 41.9% in the sample attributed to the loss of (H_2S + dien) resulting in the formation of MoS_3 (see Eq. (1)).

$$[dienH_2][MoS_4] \rightarrow H_2S + (dien) + MoS_3 \quad (1)$$

The similar observation was also reported in the literature [26]. On further treatment, a slow mass decrease was observed and the residual mass of 53.45% at 800 °C suggested the immediate formation of MoS_3 being transformed into MoS_2. The TG/DTG analysis of **I** agrees reasonably well to the molecular composition. From the TG and the DTG curve [Fig. 4(b)] of **II**, it is obvious that the decomposition reaction proceeds in three different steps, which cannot fully be resolved. The experimental mass loss is up to about 300 °C where the DTG curve shows a minimum about 39.6% which is in good agreement with the loss of the amine ligands (triethylenetetramine = 39.6%). However, the elemental analysis of the residue revealed the presence of large amounts of organic matter and therefore, it can be assumed as in the decomposition of compound **I**, the amine and H_2S are lost simultaneously. Therefore, the decomposition of compound **II** follows the following equation (2):

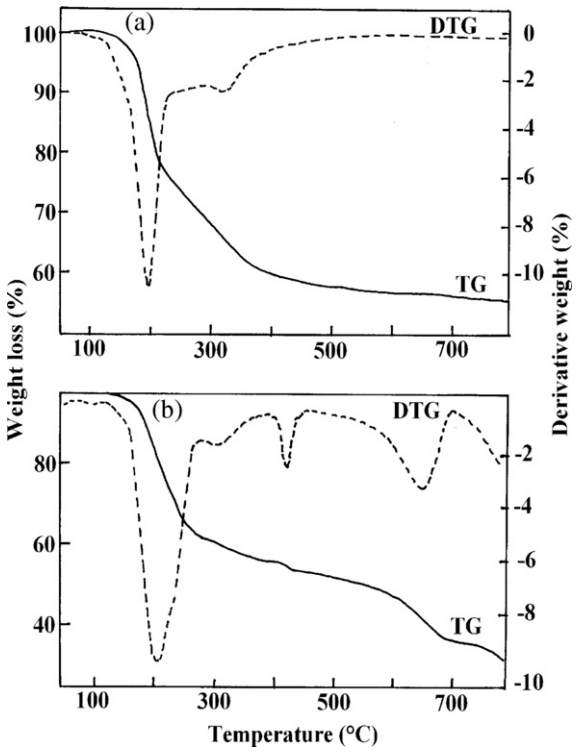

Fig. 4. TG–DTG curve of (a) [dienH_2][MoS_4] and (b) [trienH_2][MoS_4] in the range of 50–800 °C.

$$(trienH_2)[MoS_4] \rightarrow trien + H_2S + MoS_3 \quad (2)$$

The foregoing observations are summarized as follows. Crystal **I** starts decomposing at 136 °C and **II** at 175 °C whereas **III** at 190 °C. From the TG data it could be concluded latter is more thermally stable than the formers. This may also be one of the reasons why the colour of **I** changes into black in relatively lesser time than that of the **II**. The relatively stable property of **III** is due to the rigid bond structure of the bicycle amine. The morphology of the single crystals and the thermally decomposed products were studied with Scanning Electron Microscopic images [see Fig. 5 (a) and (b)]. In general, the crystals had several sediment layers indicative of the formation of the crystal planes. The micrograph of the thermal products of these crystals showed formation of capillary pores [Fig. 5(b)] within the powder. The similar capillary pores were also reported in the literature [27,28]. The formation of the pores was observed for all three samples after thermal treatment. The powder XRD of the thermal product was found to be stoichiometric MoS_2. From the XRD patterns [Fig. 6], one can see [*h k* 0] lines, but most of the [0 0 *l*] and all of the mixed [*h k l*] lines are missing indicative of a single layered MoS_2 [29]. The presence of the [1 1 0] peak in the present system suggests undistorted and symmetrical MoS_2 [30].

3.6. Differential scanning calorimetry (DSC)

Calorimetry involves the measurement of relative changes in temperature and heat energy under isothermal or adiabatic condi-

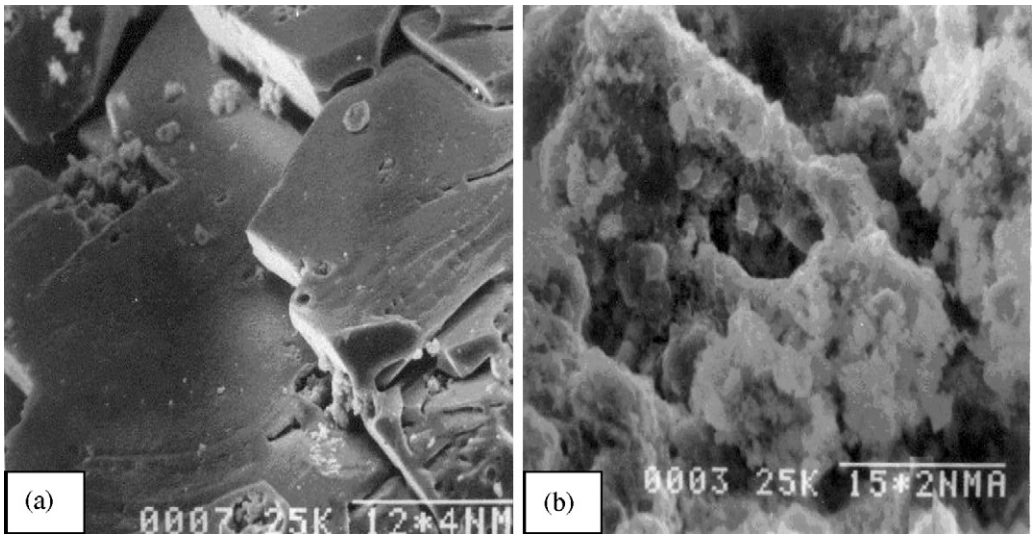

Fig. 5. Scanning electron microscopic images of the sedimented single crystals of (a) $[dienH_2][MoS_4]$ and (b) after heat treatment at 500 °C. The sedimented crystalline layers form MoS_2 porous structure in the bulk.

tions. During thermal calorimetric characterization, the adiabatic system has a significant role where the change in temperature is translated, using heat capacity of the system, into the enthalpy or energy of material. In the present thermal investigation of the organic amine-$[MoS_4]^{2-}$ single crystals, the measurement was carried out in a closed system where determination of the heat, Q, associated with a change in temperature, ΔT, yields the heat capacity (C) of the material,

$$C = \frac{Q}{\Delta T} \tag{3}$$

At constant pressure,

$$\frac{dQ}{dT} = \left[\frac{\partial H}{\partial T}\right]_{P,N} = C_p \tag{4}$$

The enthalpy, entropy and free energy is calculated from C_p through,

$$H(T) = H(T_0) + \int_{T_0}^{T_1} C_p \, dT \tag{5}$$

$$\Delta S = \int_{T_0}^{T_1} \left[\frac{C_p}{T}\right] dT \tag{6}$$

$$\Delta G = \Delta H - T\Delta S \tag{7}$$

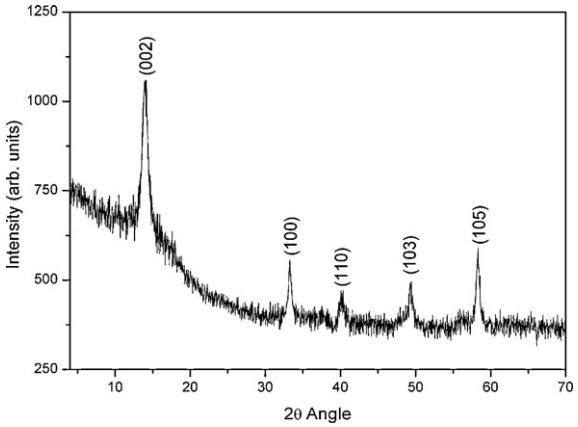

Fig. 6. Powder X-ray diffraction of the heat treated sample at 500 °C. The patterns are indicative of single layered MoS_2.

The DSC analysis for **I** was performed over the temperature range of 50–400 °C at the scanning rate of 5 °C/min. The analysis showed that the crystal was stable up to 140 °C followed by an endothermic peak in the range of 142–156 °C. This is due to the start-point decomposition of the sample with heat of decomposition being −0.05 J/g [Fig. 7(a) and (b)] at 140 °C observed by TG. The experiments were repeated thrice to ensure the reproducibility of the peaks. The sharp decomposition pattern was observed in the temperature range of 156–620 °C. The low temperature DSC measurements show the absence of transition between −170 and −60 °C. However, a series

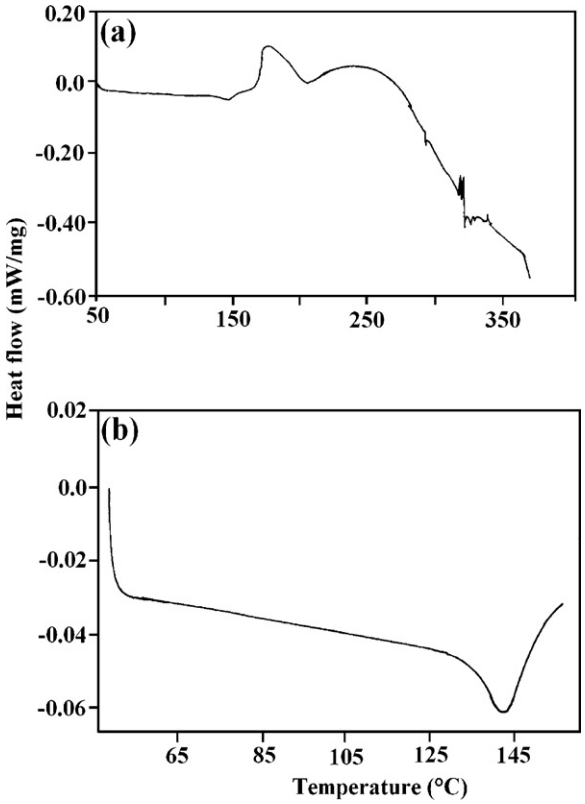

Fig. 7. (a) DSC curves of $[dienH_2][MoS_4]$ in the temperature range of 50–400 °C at the scanning rate of 5 °C/min. (b) Magnified curve in the range of 50–145 °C. The decomposition temperature was found to be 140 °C.

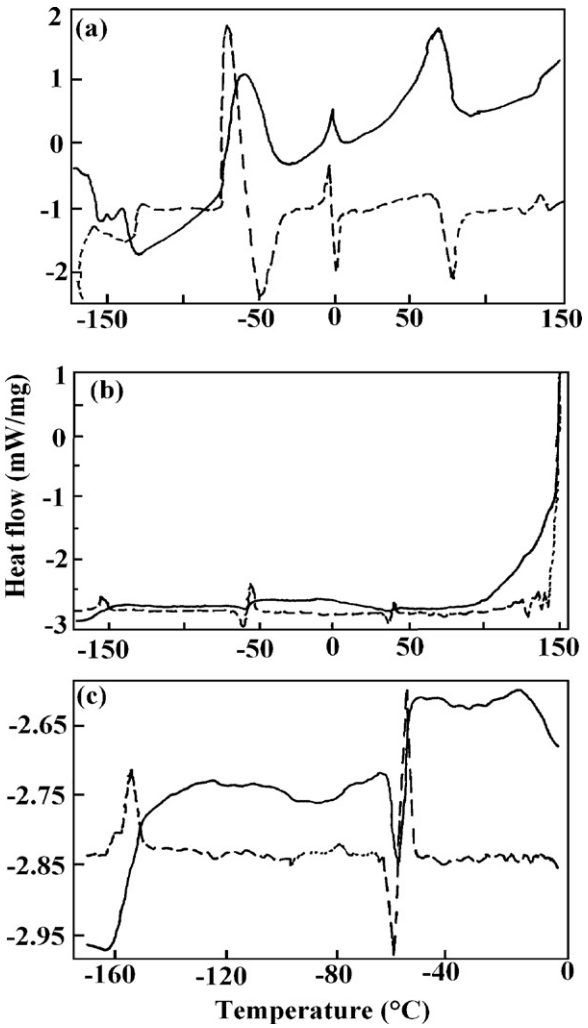

Fig. 8. The low temperature (−170 to 150 °C) DSC patterns of $[trienH_2][MoS_4]$. The single crystal was undergone heating-cooling cycles at the scanning rate of 5 °C/min.

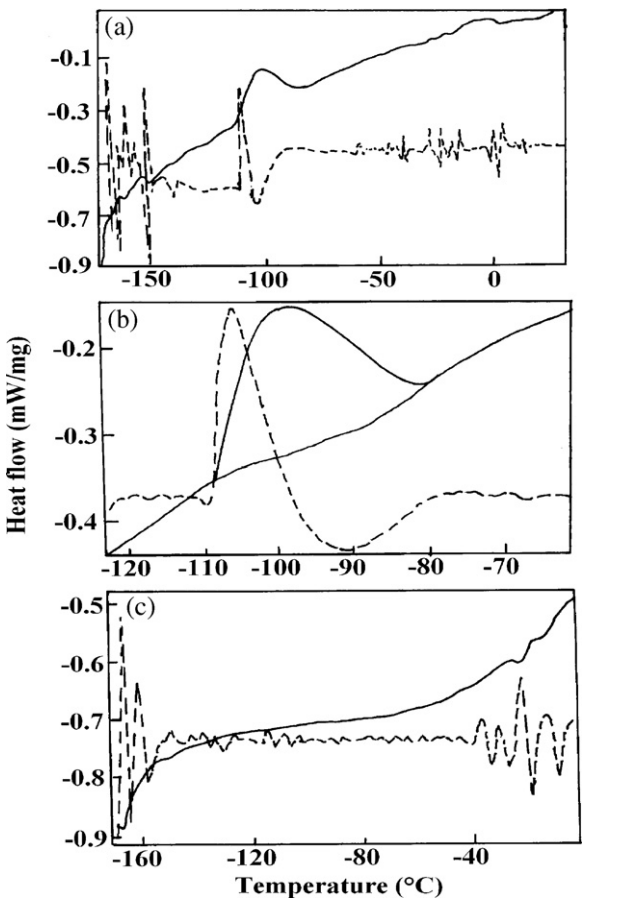

Fig. 9. The DSC patterns of $[NH_4][DABCOH][MoS_4]$. The sharp endothermic peak with ΔH of 16.58 J/g at the temperature of −100 °C in the temperature intervals of −110 to −80 °C was found to be due to melting.

of endothermic peaks were observed at −61, 0 and 72 °C as well as glassy transition at 140 °C with the corresponding ΔH values of 8.32, 2.99, 24.08, and 0.21 J/g respectively (Fig. 8(a)–(c)). The ΔH, C_p, ΔS and ΔG at different transitions could easily be determined using Eqs. (3)–(7). The sharp endothermic DSC peak at −61 °C is due to solid transition during the heat scanning. For a solid-state transition to occur, the peaks should be sharp and reversible. The melting endotherms for pure substances are very sharp, i.e. they occur [31] over a narrow temperature interval and the melting point T_m is usually determined from the peak. However, in the present case, the peaks are spread over a wider interval of temperature though the peaks are sharp. In order to explain the reversibility of a solid-state transition in **II** the peaks (−61, 0 and 72 °C) observed during heating were also observed at (−58, 0 and 70 °C) during cooling. It is suggested that the sample has undergone reversible solid phase transition at these three temperatures and due to the unavailability of in situ XRD, the phases could not be identified. The DSC studies of **III** showed one sharp endothermic peak [Fig. 9(a)–(c)] with ΔH ∼16.58 J/g at the temperature of −100 °C in the temperature intervals of −110 to −80 °C which is due to melting. On further scanning, the three small exothermic transitions followed by one small endothermic transition with ΔH ∼−0.5537, −0.1308, −1.074 and 0.391 J/g are obtained over the temperature range of −26, −21, −13 and +5 °C respectively. The series of peaks at these temperatures is an indication of solid-state transitions in the sample while heat scanning. Furthermore, when the sample was cooled, several transitions at different temperatures were obtained. The exothermic reversible transitions at −167, −163, −151, −143, −130 and −114 °C have ΔH value ∼−1.34, −0.756, −0.097, −0.080 and −0.124 J/g and one endothermic transition at −131 °C has the ΔH value of 0.141 J/g. It was found that the peaks in the heating and cooling cycles were reversible to one another even after three cycles of scanning. The low temperature thermal events studied with DSC experiments highlight the complex thermal behavior of the crystals.

4. Conclusions

Water soluble amine-MoS_4 hybrid single crystals have been prepared and characterized using several analytical techniques. The differences in the molecular structure have been explained considering the variation in the hybridisation characters. The crystals have very complex decomposition patterns at high temperature and several solid-solid transitions at low temperature. The comparison between the two linear hybrid molecules and cyclic hybrid molecule shows that former has relatively lower decomposition temperature and lower stability in air compared to the former (rigid bicyclic-MoS_4) crystal. These Mo–S based water soluble based single crystals could be tailored for the building blocks of heterobinuclear structures for improvement towards metastatic cancer.

Acknowledgements

Suman Pokhrel would like to thank Jawaharlal Nehru Memorial Fund (ref:su/3/1/2000/601) for the financial support to carry out

this work in the Department of Chemistry, Loyola College, Chennai, during 2000–2002.

References

[1] B.R. Srinivasan, S.V. Girkar, C. Näther, W. Bensch, J. Coord. Chem. 62 (2009) 3559.
[2] M. Hofman, Inorg. Chem. 47 (2008) 5546.
[3] Z.-D. Huang, W. Bensch, L. Kienle, S. Fuentes, G. Alonso, C. Ornelas, Catal. Lett. 127 (2009) 132.
[4] B.G. Alberding, M.H. Chisholm, Y.-H. Chou, Y. Ghosh, T.L. Gustafson, Y. Liu, C. Turro, Inorg. Chem. 48 (2009) 11187.
[5] J.P. Donahue, Chem. Rev. 106 (2006) 4747.
[6] B.R. Srinivasan, A.R. Naik, M. Poisot, C. Näther, W. Bensch, Polyhedron 28 (2009) 1379.
[7] V.M. Cornel, J. Org. Chem. 73 (2008) 2960.
[8] R. Frantz, E. Guillamon, J. Lacour, R. Llusar, V. Polo, C. Vincent, Inorg. Chem. 46 (2007) 10717.
[9] A.M. Appel, S.-J. Lee, J.A. Franz, D.L. DuBois, M.R. DuBois, J.C. Birnbaum, B. Twamley, J. Am. Chem. Soc. 130 (2008) 8940.
[10] G. Schwarz, R.F. Mendel, M.W. Ribbe, Nature 460 (2009) 839.
[11] Y. Zang, V.N. Gladyshev, J. Mol. Biol. 379 (2008) 881.
[12] S. Groysman, R. Holm, Biochemistry 48 (2009) 2310.
[13] C. Léger, P. Bertrand, Chem. Rev. 108 (2008) 2379.
[14] R.A. Rothery, G.J. Workun, J.H. Weiner, Biochim. Biophys. Acta 1778 (2008) 1897.
[15] H.I. Pass, G.J. Brewer, R. Dick, M. Carbone, S. Merajver, Ann. Thorac. Surg. 86 (2008) 383.
[16] B. Hassouneh, M. Islam, T. Nagel, Q. Pan, S.D. Merajver, T.N. Teknos, Mol. Cancer Ther. 6 (2007) 1039.
[17] S. Pokhrel, K.S. Nagaraja, B. Varghese, J. Chem. Crystallogr. 33 (2003) 903.
[18] S. Pokhrel, K.S. Nagaraja, B. Varghese, J. Struct. Chem. 44 (2003) 689.
[19] S. Pokhrel, K.S. Nagaraja, B. Varghese, J. Struct. Chem. 45 (2004) 900.
[20] J. Chandrasekharan, M.A. Ansari, S. Sarkar, J. Less Common Met. 134 (1987) L23.
[21] S. Pokhrel, PhD thesis, University of Madras, 2003.
[22] J. Han, D. Coucouvanis, Inorg. Chem. 41 (2002) 2738.
[23] R. Dessapt, C. Simonnet-Jegat, J. Marrot, F. Secheresse, Inorg. Chem. 40 (2001) 4072.
[24] J.E. Combariza, J.H. Enemark, M. Barfield, J.C. Facelli, J. Am. Chem. Soc. 111 (1989) 7619.
[25] S. Kulpe, D. Dähne, Acta Cryst. B 34 (1978) 3616.
[26] B.R. Srinivasan, J. Chem. Sci. 116 (2004) 251.
[27] B.R. Srinivasan, S.N. Dhuria, M. Poisot, C. Nather, W. Bensch, Z. Naturforsch. 59b (2004) 1083.
[28] M. Poisot, W. Bensch, Thermochim. Acta 453 (2007) 42.
[29] J.V. Lauritsen, J. Kibsgaard, S. Helveg, H.T. Oslashe, B.S. Clausen, E.L. Gaard, F. Besenbacher, Nat. Nanotechnol. 2 (2007) 53.
[30] D. Yang, S.J. Sandoval, W.M.R. Divigalpitiya, J.C. Irwin, R.F. Frindt, Phys. Rev. B 43 (1991) 12053.
[31] P.J. Sanchez, J.M. Gines, M.J. Arias, C.S. Novak, A. Rniz-Londe, J. Therm. Anal. Calorim. 67 (2002) 189.